On SAR-Based Statistical Ice Thickness Estimation in the Baltic Sea

Markku Similä[1], Juha Karvonen[1], Martti Hallikainen[2], Christian Haas[3]
[1] Finnish Institute of Marine Research (FIMR), PB 33, FIN-00931, Helsinki, Finland
[2] Helsinki Univ. of Technology, Laboratory of Space Technology (HUT/LST), Finland
[3] Alfred Wegener Institute (AWI), Bremerhaven, Germany
Email: Markku.Simila@fimr.fi

I. Introduction

In the Baltic Sea the annual maximum ice extent varies strongly, from the minimum (12 %) to an almost total ice cover over the Baltic Sea, the average being 40 % during the last 30 years. The occurrence of such large annual ice cover has guided the SAR based sea ice mapping work done at the Finnish Institute of Marine Research (FIMR). During the winters 2003-2005 ice thickness measurement campaigns with a simultaneous acquisition of satellite-borne SAR data have been performed. Using these data sets we can address the problem how well one can estimate ice thickness or some other quantity related to it using solely SAR data. In this paper some estimation results for a 1-dimensional data set are presented. In our other paper [1] an approach to the estimation in the two dimensional setting, a much harder problem, is described. Here we will examine the applicability of two different quantities describing the total sea ice thickness. The quantities are: total ice thickness (T) and equivalent deformed ice thickness (T_{def}). The proposed methods use either a classification or a regression approach.

The surface scattering dominates the backscattering at C-band [2]. The link between the ice thickness and the backscattering strength is surface roughness. Typically the surface of level ice becomes more rough when aging due to weathering. Hence, the radar response is, on average, stronger from older (and thicker) level ice than from newer (and thinner) level ice. A major exception for this correspondence is the fast ice area where the thickest level ice fields occur. For many reasons, e.g. for snow ice, the surface roughness and ice thickness in the fast ice field are so weakly correlated that there does not exist any functional relationship between them. Another major exception is the marginal ice zone. In the sequel we restrict our analysis only to the estimation of ice thickness in drift ice areas, excluding fast ice and marginal ice zones, see [1]. The most drastic changes in the ice thickness are associated with the deformation of ice fields, i.e. the formation of ice ridges or hummocks. Both these deformation types significantly modify the ice surface characteristics. Hence, these deformed areas can be detected by SAR, the detection accuracy being dependent on the resolution of the sensor.

II. Data

In 2004, sea ice thickness measurements using helicopter-borne electromagnetic induction (EM) based ice thickness measurements instrument were performed by Alfred Wegener Institute (AWI) in the Gulf of Bothnia. These measurements were complemented by the acquisition of ENVISAT precision mode (IMP) ASAR images, which were acquired on the same day as the EM measurement flights were made. Hence, we have data sets consisting of the pairs (T, y), where T is the ice thickness measurement and y the corresponding SAR intensity value.

The data sets are in different resolutions, the sampling rate of the EM measurement is 3-4 m and the EM measurement resolution is around 20-30 m, and the ENVISAT images are in 30 m resolution. The comparisons are additionally complicated by uncertainties related to the registration inaccuracies between the data sets which were partly caused by ice field movement between the data acquisitions. A reasonable way to compare these kind of data sets is to make statistical comparisons. Our material covers 8 ASAR images, and about 920 km of EM flight lines in total. The EM measurements were conducted in two campaigns over a highly ridged drift ice area between February 10th and May 14th 2004 in Gulf of Bothnia.

There occurs an underestimation bias in the EM based ice thickness measurements of ridges due to the nature of the measurement technique. The ice thickness is determined using the altitude with respect to the sea water. This may lead to even 50 % underestimation of a true ice ridge thickness, depending on the geometry and and consolidation of ridge keel [3].

The mean daily temperatures during the EM measurement campaigns were typically below zero degrees, although on three days the maximum temperature rose above zero degrees. Hence, this data set represents a relatively wide range of snow moisture variation.

Incidence angle of an illuminating radar wave influences the strength of the backscattering. For RADARSAT data, we have obtained enough scenes to determine a scaling factor, which normalizes the SAR pixel values to roughly correspond a fixed incidence angle [4]. For ENVISAT data, we treat different incidence angle ranges separately. In the current data set we regard the incidence angle to be low, if it varies between $19-25$ degrees, and high for $26-34$ degrees range.

III. Estimation procedure

A. Ice thickness characteristics

The obtained results are based on the following characterization of sea ice types. On the basis of the EM measurements, the ice fields were divided into four different categories: level ice class consisting of ice fields with a thickness less than 50 cm (the upper limit for the estimated maximum thermal ice growth) rafted ice (thickness range from 50 cm to 100 cm), small ridges (thickness from 101 cm to 200 cm) and large ridges (thickness over 2 m). The first two classes are rather

0-7803-9051-2/05/$20.00 (C) 2005 IEEE

obvious. The ridges were divided into two subclasses because it was assumed that the larger ridges can be more easily detected from their surrounding than the small ridges. The mean ice thicknesses of the respective classes are computed from the training samples.

It is not clear that the best results are achieved by directly relating the radar intensity and the ice thickness. The correspondence between the backscattering intensity may be better for some other ice parameter related to the ice thickness. Here we have also examined the estimation accuracy for the equivalent deformed ice thickness (T_{def}).

The total (mean over a segment) ice thickness (T) is the sum of the level ice thickness (T_{lev}) and equivalent deformed ice thickness:

$$T = T_{lev} + T_{def}. \tag{1}$$

The quantity T_{def} depicts the thickness of the hypothetical ice field, if the the ridged ice were to be spread uniformly over the area to be surveyed. Such an account of ridges is sensible only on scale larger than a few kilometers. We used segments with a length of 3 km in the computation. A disadvantage of this approach is that one must also have an estimate for T_{lev}. In our analysis this was obtained directly from the EM measurements, as a segment mean of the EM measurements below 50 cm. In practice, one can use the digitized ice chart to get this information.

B. Estimation

We use the MAP-classifier, which assigns a SAR pixel y to the class k, $\quad k \in \{1, \ldots, 4\}$ with a maximum a posterior probability. These probabilities are computed according to the formula

$$Pr(C = k|Y = y) = \frac{p_k f_k(y)}{\sum_{l=1}^{4} p_k f_k(y)}, \tag{2}$$

where $Pr(C = k|Y = y)$ is the posterior probability of the class k given the intensity value y, f_k is the class-wise kernel density estimate obtained with a Gaussian kernel, and p_k is the prior probability of the class k.

To take into account the location inaccuracies between the data sets, we used the SAR intensity values y computed over 9x9 pixel windows (270 m by 270 m) in SAR images. Due to the large variation of the backscattering coefficient in each ice class, the results are reported for segments with a length of about 3 km, i.e. a segment with 1000 EM samples T_i. Also the use of quantity T_{def} requires this.

In the estimation we proceed as follows. Every y_i is assigned to some ice class, say k, according to the MAP rule. Then the thickness estimate $\hat{T}_i$ given y_i is the median thickness of the class k. These values were determined from a training set. For our training data they were 25 cm, 72 cm, 140 cm and 240 cm, respectively. Finally, the mean of the pixel-wise estimates is taken as an estimate for the mean ice thickness over the segment, i.e. over the 1000 thickness estimates. As the ground truth we use the means of the respective EM measurements.

We also tested the following modification. Given y_i, $\hat{T}_i$ was computed as a weighted average of the class-wise mean ice thicknesses, where the weight for each class is the corresponding posterior probability. This approach can be considered as a way to directly model the ice thickness estimate as a regression function of the backscatter. The fitting was carried out separately for each discrete σ^0 value (range from -25 dB to -8 dB), without using a global criterion (like least squares minimization). The resulting regression curve is almost linear, see [1].

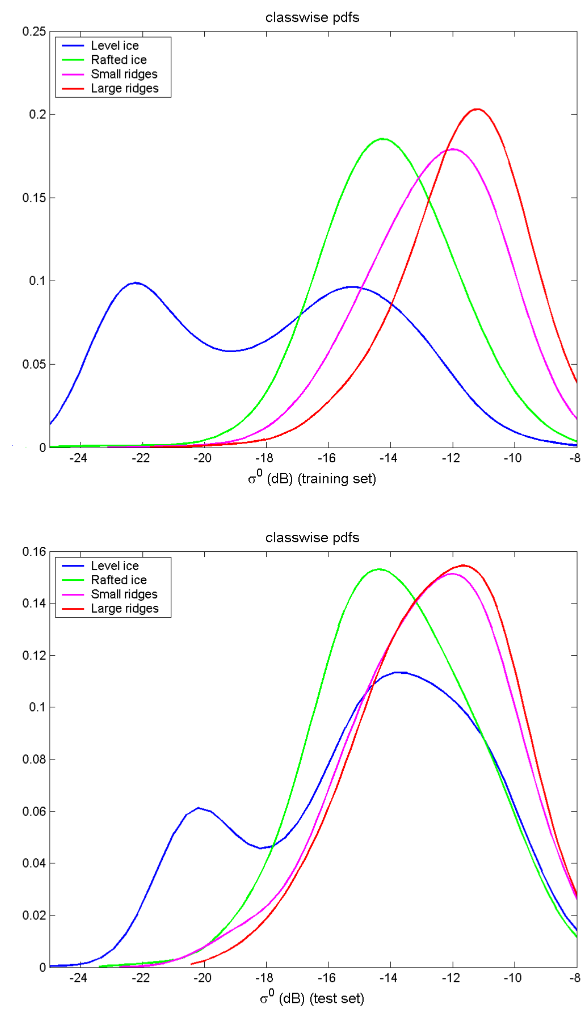

Fig. 1. The class-wise probability densities using only SAR measurements in the high incidence angle range. In the upper panel are the densities for the training set, in the lower for the test set.

IV. Results

We used the first half of the EM measurements as a training set. The backscattering strength is very sensitive to the incident angle. Because we had only relatively few low incidence angle measurements at our disposal, only high incidence angle SAR values were used in the training. As we can see from Fig. 1, the class separability in the training set was good. The opposite holds for the test set, where a relative large fraction of the level ice EM measurements had a large σ^0 value. This is a surprising feature and difficult to explain geophysically. One is tempted to think that it is due to registration inaccuracies

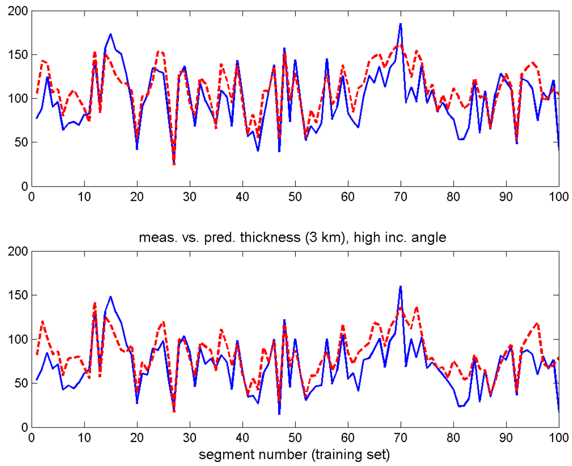

Fig. 2. The estimation results computed with the regression approach (high incidence angle range, training set). Results for T in upper panel, for T_{def} in lower panel.

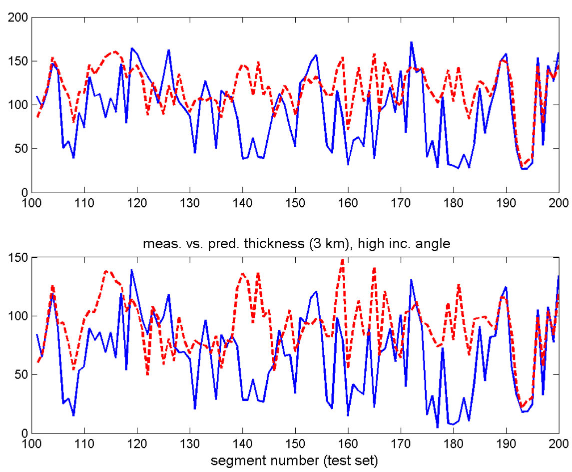

Fig. 3. The estimation results computed with the regression approach (high incidence angle range, test set). Results for T in upper panel, for T_{def} in lower panel.

between data sets. Anyway, the high backscatter originating from level ice gives one a reason to assess the test results with caution.

The estimation results are collected in Table I. The used error measure was the mean of the absolute differences between the segment-wise estimates and the EM measurements, i.e. l_1 error. One can see that the results for the training set were good using both the approaches. On other hand, the results for the test set were rather poor. By inspecting the occurrence of large errors, one can observe that the proposed approaches could not detect the level ice areas around the segment number 140 (in the test set) and neither the level ice areas around the segment number 180. Otherwise, the estimates to some extent followed the EM measurements. It is of interest to note that even if the systematic errors were large for the low incidence angle range measurements, the estimation bias remained almost constant

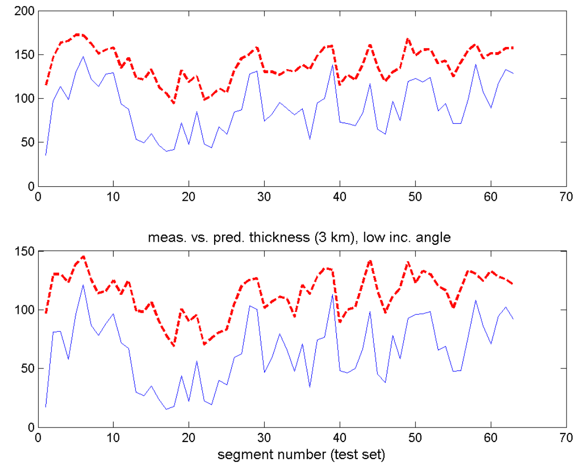

Fig. 4. The estimation results computed with the regression approach (low incidence angle range, test set). Results for T in upper panel, for T_{def} in lower panel.

TABLE I

ESTIMATION ERROR. l_1 ERROR MEASURE (BIAS INSIDE BRACKETS). LOW RANGE REFERS TO LOW INC. ANGLE MEASUREMENTS.

Algorithm	Data set	T (cm)	T_{def} (cm)
Regression	Train	19.8 (-14.4)	19.3 (-14.6)
	Test	37.6 (-29.8)	36.8 (-29.7)
	Low range	39.0 (-35.7)	38.5 (-35.4)
Classifi-cation	Train	26.3 (-20.5)	25.6 (-19.5)
	Test	44.2 (-33.7)	43.2 (-32.8)
	Low range	50.9 (-48.2)	50.0 (-47.3)

for all the segments. On the basis of this, one can expect rather good results for this incidence angle range when enough data representing this incidence angle range has been gathered.

The results based on the regression were slightly better than for the classification approach. No evidence was found to prefer T_{def} over T.

In the future we will examine the empirical estimation of the prior probabilities used in the computations.

REFERENCES

[1] J. Karvonen, M. Similä, M. Hallikainen, C. Haas, Estimation of Equivalent Deformed Ice Thickness from Baltic Sea Ice SAR Imagery, Proc. IEEE International Geoscience and Remote Sensing Symposium 2005 (IGARSS'05), 2005.

[2] A. Carlström and L.M.H. Ulander, "Validation of backscatter models for level and deformed sea ice in ERS-1 SAR images," Int. Journal of Remote Sensing, vol. 16, no. 7, pp. 3245-3266, 1995.

[3] C. Haas, Airborne EM Sea-Ice Thickness Profiling over Brackish Baltic Sea Water, in Proc. of the International Symposium on Ice St. Petersburg, 2004.

[4] M. Mäkynen, T. Manninen, M. Similä, J. Karvonen, M. Hallikainen, Incidence Angle Dependence of the Statistical Properties of the C-Band HH-Polarization Backscattering Signatures of the Baltic Sea Ice, IEEE Tansactions on Geoscience and Remote Sensing, vol 40, n 12, pp. 2593-2605, 2002.